



Contents lists available at ScienceDirect

## Journal of Materials Science &amp; Technology

journal homepage: [www.jmst.org](http://www.jmst.org)

## Phase Selection in Solidification of Undercooled Co–B Alloys

X.X. Wei<sup>1</sup>, W. Xu<sup>2</sup>, J.L. Kang<sup>1</sup>, M. Ferry<sup>2</sup>, J.F. Li<sup>1,\*</sup><sup>1</sup> State Key Laboratory of Metal Matrix Composites, School of Materials Science and Engineering, Shanghai Jiao Tong University, Shanghai 200240, China<sup>2</sup> Australian Research Council Centre of Excellence for Design in Light Metals, School of Materials Science and Engineering, The University of New South Wales, Sydney, NSW 2052, Australia

## ARTICLE INFO

## Article history:

Received 13 December 2015

Received in revised form

25 January 2016

Accepted 27 January 2016

Available online

## Key words:

Undercooling

Rapid solidification

Metastable phase diagram

Structure evolution

A series Co–(18.5–20.7) at.% B melts encompassing the eutectic composition (Co<sub>81.5</sub>B<sub>18.5</sub>) were solidified at different degrees of undercooling. It is found that the metastable Co<sub>23</sub>B<sub>6</sub> phase solidifies as a substitute for the stable Co<sub>3</sub>B phase in the alloy melts undercooled above a critical undercooling value of ~60 K. The Co<sub>23</sub>B<sub>6</sub> and  $\alpha$ -Co phases make up a metastable eutectic. The corresponding eutectic composition and temperature are Co<sub>80.4</sub>B<sub>19.6</sub> and 1343 K, respectively. On exposure of the metastable Co<sub>23</sub>B<sub>6</sub> phase at a given temperature above 1208 K, it does not decompose even after several hours. But it transforms by a eutectoid reaction to  $\alpha$ -Co + Co<sub>3</sub>B at lower temperature.

Copyright © 2016, The editorial office of Journal of Materials Science & Technology. Published by Elsevier Limited.

## 1. Introduction

Solidification structure changes with the melt undercooling prior to solidification. A high undercooling can be achieved by either rapidly quenching the melt or excluding heterogeneous nucleation substrates from it. In the first case, one is difficult to trace the thermo-physical properties associated with crystal nucleation and growth. In the latter, however, it becomes possible to monitor the temperature recalescence behavior. With the obtained information, a number of high-undercooling induced phenomena, such as the grain refinement in single phase alloys<sup>[1–5]</sup>, the transition from lamellar to anomalous eutectic in eutectic alloys<sup>[6–9]</sup> and metastable phase formation<sup>[10–13]</sup> have been well interpreted. More importantly, bulk non-equilibrium materials can be produced by the latter method.

M–B (M = Fe, Ni, Co) alloys are widely used as soft magnetic materials. A comprehensive understanding of their structure evolution with undercooling is very important for improving the soft magnetic properties. So far explorations were mainly performed on the solidification behavior of Ni–B<sup>[14–16]</sup> and Fe–B<sup>[17–19]</sup> alloys, which resulted in the discovery of metastable Ni<sub>23</sub>B<sub>6</sub> and Fe<sub>3</sub>B phases at high undercooling. Unfortunately, the Ni<sub>23</sub>B<sub>6</sub> phase is so unstable that it decomposes and transforms into stable Ni and Ni<sub>3</sub>B phases during the subsequent cooling, which hinders the structural investigation

of metastable Ni<sub>23</sub>B<sub>6</sub> phase. Recently, Ohodnicki et al.<sup>[20]</sup> simulated the crystal structure and energy of possible phases in M–B alloys, and predicted that metastable M<sub>23</sub>B<sub>6</sub> phase is relatively stable in Co–B binary alloys than that in Fe–B and Ni–B binary alloys. Thus, a special solidification structure evolution associated with metastable Co<sub>23</sub>B<sub>6</sub> phase formation may be present in Co–B alloys. In this paper, we report the experimental results of the solidification behavior of undercooled Co–B alloys.

## 2. Experimental Procedures

The Co-rich side of the Co–B phase diagram contains both a eutectic reaction  $L \rightarrow \alpha\text{-Co} + \text{Co}_3\text{B}$  at 18.5 at.% B, and a peritectic reaction  $L + \text{Co}_2\text{B} \rightarrow \text{Co}_3\text{B}$  at 25 at.% B. A series of alloys around the eutectic composition (Co<sub>81.5</sub>B<sub>18.5</sub>) were selected for investigation. The alloys were synthesized from 99.999 wt% Co and B blocks. To minimize errors in alloy composition caused by the volatilization of B during melting, a Co<sub>75</sub>B<sub>25</sub> master alloy was initially produced. Ingots of various compositions around the eutectic composition were prepared by arc melting a mixture of high purity Co and the master alloy under a high purity argon atmosphere on a water-cooled copper hearth. Each ingot was remelted several times and turned over after each solidification stage to ensure chemical homogeneity.

For the undercooling experiments, about 3 g of a given alloy and a small quantity of B<sub>2</sub>O<sub>3</sub> glass flux were put together into a fused silica crucible and inserted in the induction-heating coil. The flux was dehydrated for 6 h at 1273 K before use. After evacuating the

\* Corresponding author. Fax: +86 21 54748530.

E-mail address: [jfli@sjtu.edu.cn](mailto:jfli@sjtu.edu.cn) (J.F. Li).

vacuum chamber to a pressure of  $2 \times 10^{-3}$  Pa, ultra-high purity argon was back-filled into the chamber, followed by induction melting of each alloy. Covered by the molten flux, each alloy was cyclically superheated and cooled until a desired undercooling was obtained. Each alloy was then cooled to room temperature. An infrared pyrometer with an accuracy of 1 K and a response time of 1 ms was utilized to monitor the thermal history of each alloy, with the subsequent temperature data recorded in a computer. To avoid interfering with nucleation, solidification was designed to take place spontaneously rather than triggered manually.

Each solidified alloy was sectioned, polished, and etched with a mixture of glacial acetic acid, hydrochloride acid, nitric acid and water. The solidification microstructures were analyzed using a JSM7600F field emission gun scanning electron microscope (SEM), and the composition of the phases determined by energy dispersive spectroscopy (EDS). The phase constitution of the alloys was determined using a Thermo ARL X-ray diffractometer (XRD).

Thermal analysis was performed in a Netzsch (404F3) differential scanning calorimeter (DSC) under a flow of high-purity argon. The temperature and enthalpy of the instrument were calibrated with pure In, Sn, Bi, Zn, Al and Au. A given sample weighing ~10 mg was placed in an alumina crucible and subject to two types of thermal processing: (i) the alloys were heated isochronally until completely melted, followed by cooling both at a rate of 20 K/min to determine the characteristic temperatures associated with any phase transformations that occur, and (ii) the molten alloys were cooled rapidly at a rate of 40 K/min from the liquidus temperature to a pre-determined temperature, and then held isothermally for up to several hours to investigate the stability of  $\text{Co}_{23}\text{B}_6$ .

### 3. Results and Discussion

#### 3.1. Solidification of Co–B alloys around the eutectic composition

The  $\text{L} \rightarrow \alpha\text{-Co} + \text{Co}_3\text{B}$  equilibrium eutectic reaction was first investigated. Fig. 1 shows the DSC curves of a hypoeutectic, eutectic and hypereutectic alloy, which were solidified under near-equilibrium conditions (<5 K undercooling). The curve of  $\text{Co}_{81.5}\text{B}_{18.5}$  is composed of a single endothermic peak whereas the curves of both  $\text{Co}_{83.7}\text{B}_{16.3}$  and  $\text{Co}_{80.4}\text{B}_{19.6}$  have two partially overlapping peaks, indicating that  $\text{Co}_{81.5}\text{B}_{18.5}$  is the eutectic composition, as confirmed in

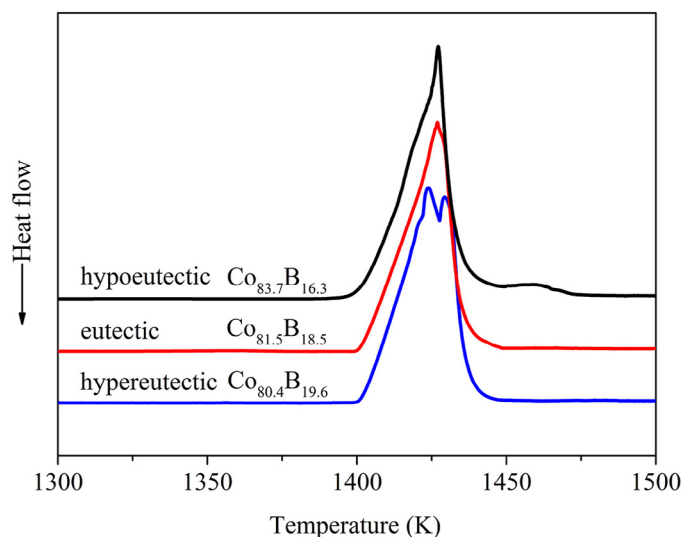


Fig. 1. Heating DSC curves of hypoeutectic, eutectic and hypereutectic alloy samples solidified at an undercooling below 5 K (heating rate = 20 K/min).

the phase diagram<sup>[21]</sup>. However, all alloys started to melt at 1403 K, which corresponds to a higher temperature than the reported eutectic temperature of 1383 K<sup>[21]</sup>. As the superheating of a solid during melting is negligible, the equilibrium eutectic temperature of the Co–B alloys should therefore be 1403 K. The difference between the published eutectic temperature in 1966<sup>[22]</sup> and the present analysis may be due to improvements in the accuracy of analysis. Hereafter, we use 1403 K as the equilibrium eutectic temperature.

The solidification microstructure of the Co–B alloys changes significantly with the melt undercooling prior to nucleation. Fig. 2 shows the microstructure of  $\text{Co}_{81.5}\text{B}_{18.5}$  eutectic alloy solidified at various degrees of undercooling. A lamellar eutectic forms when the undercooling is less than 60 K (Fig. 2(a and b)); the dark phase and gray matrix phase are  $\alpha\text{-Co}$  and  $\text{Co}_3\text{B}$ , respectively. At larger undercooling (up to a maximum of 75 K in the present work), primary  $\alpha\text{-Co}$  dendrites are surrounded by another phase, with a very fine fibrous eutectic filling the remaining space (Fig. 2(c and d)). To understand why an abrupt microstructural change occurs at some critical undercooling, the eutectic alloy was solidified at an undercooling of 55 and 65 K, respectively, and examined by XRD as shown in Fig. 2(e). It can be seen that the alloy consists of  $\alpha\text{-Co}$  and  $\text{Co}_3\text{B}$  at 55 K undercooling, whereas  $\alpha\text{-Co}$  and  $\text{Co}_{23}\text{B}_6$  form at 65 K undercooling. Hence, the unidentified gray phase surrounding the primary  $\alpha\text{-Co}$  dendrites at large undercooling (Fig. 2(c and d)) is  $\text{Co}_{23}\text{B}_6$ , with the remaining space comprised of the  $\alpha\text{-Co}/\text{Co}_{23}\text{B}_6$  eutectic. That is to say, solidification of the  $\text{Co}_{81.5}\text{B}_{18.5}$  eutectic alloy at an undercooling greater than 60 K generates metastable  $\text{Co}_{23}\text{B}_6$  rather than stable  $\text{Co}_3\text{B}$ .

Temperature recalescence is a useful indicator of the solidification behavior of an alloy. Fig. 2(f) shows the cooling curves for the eutectic alloy at various degrees of undercooling. For an undercooling less than 60 K, there is a single temperature recalescence event during solidification with the highest recalescence temperature approaching the eutectic temperature (1403 K). However, for an undercooling greater than 60 K, there is a significant change in recalescence behavior with two recalescence events appearing on the cooling curves. During the first recalescence event, the alloy is reheated to a temperature far below the eutectic temperature. The alloy then starts to cool but is disrupted by a secondary recalescence event. Interestingly, the highest temperature reached during the secondary recalescence is essentially the same for all alloy compositions, which is followed by an extended temperature plateau before a more rapid decrease in temperature.

Based on these results, a relationship between the degree of undercooling and solidification path is established for the  $\text{Co}_{81.5}\text{B}_{18.5}$  eutectic alloy. For small undercooling (<60 K), the alloy solidifies into a classic  $\alpha\text{-Co}/\text{Co}_3\text{B}$  lamellar eutectic. At large undercooling, the metastable  $\text{Co}_{23}\text{B}_6$  phase substitutes  $\text{Co}_3\text{B}$  during solidification. In this situation, the first recalescence event is associated with the rapid growth of primary  $\alpha\text{-Co}$ . As this phase grows in the liquid in the time interval between the two recalescence events, the B atoms rejected from the solid due to solute redistribution enrich the liquid ahead of the interface. The metastable  $\text{Co}_{23}\text{B}_6$  phase then nucleates and rapidly grows in this B-rich liquid, resulting in the secondary temperature recalescence event, which eventually forms a solidification structure of primary  $\alpha\text{-Co}$  dendrites surrounded by a halo of this metastable  $\text{Co}_{23}\text{B}_6$  phase. This phenomenon, where halos of one eutectic phase encompass another eutectic phase, is widely observed in the solidification microstructure of off-eutectic composition alloys<sup>[23–26]</sup>. With the composition of the remaining liquid changing back to the eutectic composition owing to the  $\text{Co}_{23}\text{B}_6$  phase growth, the remaining liquid transforms into a fibrous  $\alpha\text{-Co}/\text{Co}_{23}\text{B}_6$  eutectic during the following period of the temperature plateau. The formation of primary  $\alpha\text{-Co} + \alpha\text{-Co}/\text{Co}_{23}\text{B}_6$  eutectic in the deeply undercooled eutectic  $\text{Co}_{81.5}\text{B}_{18.5}$  alloy melt indicates that the

Download English Version:

<https://daneshyari.com/en/article/5451651>

Download Persian Version:

<https://daneshyari.com/article/5451651>

[Daneshyari.com](https://daneshyari.com)